Robotica: (2020) volume 38, pp. 88–105. © Cambridge University Press 2019
doi:10.1017/S0263574719000481

Design and Manufacturing of Tendon-Driven Soft Foam Robots

Nikolas Kastor†*, Ritwika Mukherjee§, Eliad Cohen‡, Vishesh Vikas¶, Barry A. Trimmer§ and Robert D. White†

† *Department of Mechanical Engineering, Tufts University, Medford, MA, USA.*
E-mail: r.white@tufts.edu
§ *Department of Biology, Tufts University, Medford, MA, USA.*
E-mails: Ritwika.Mukherjee@tufts.edu, Barry.Trimmer@tufts.edu
‡ *Department of Biomedical Engineering, University of Massachusetts, Lowell, MA, USA.*
E-mail: eliadcohen@gmail.com
¶ *Department of Mechanical Engineering, University of Alabama, Tuscaloosa, AL, USA.*
E-mail: vvikas@eng.ua.edu

(Accepted March 12, 2019. First published online: May 15, 2019)

SUMMARY
A design and manufacturing method is described for creating a motor tendon–actuated soft foam robot. The method uses a castable, light, and easily compressible open-cell polyurethane foam, producing a structure capable of large (∼70% strain) deformations while requiring low torques to operate (<0.2 N·m). The soft robot can change shape, by compressing and folding, allowing for complex locomotion with only two actuators. Achievable motions include forward locomotion at 13 mm/s (4.3% of body length per second), turning at 9°/s, and end-over-end flipping. Hard components, such as motors, are loosely sutured into cavities after molding. This reduces unwanted stiffening of the soft body. This work is the first demonstration of a soft open-cell foam robot locomoting with motor tendon actuators. The manufacturing method is rapid (∼30 min per mold), inexpensive (under $3 per robot for the structural foam), and flexible, and will allow a variety of soft foam robotic devices to be produced.

KEYWORDS: Soft robotics; Foam; Prototyping; Polyurethane foam; Manufacturing

1. Introduction

Soft-bodied robots are a potentially disruptive technology for applications such as human–machine interaction, low-force grasping, medical diagnostic and therapy, disaster relief, search-and-rescue, structure inspection, and surveillance. In contrast to traditional robots constructed from stiff materials, soft robots have the potential to negotiate environments by changing shape and dimensions (e.g., folding)[1,2] while exerting low contact forces and resisting damage from sudden impacts. These capabilities have motivated the development of several types of soft robot platforms as described in these review papers.[3–6]

All of the robots exhibited in refs. [3–6] have introduced soft materials in one way or another. Many examples use low-modulus but nearly incompressible polymers. Therefore, in order to achieve compressibility, or large deformation buckling, continuous structures with slots, cutouts, or long bending elements are generally required.[7,8] An alternative material – which has not been fully explored and may offer advantages due to its continuous structure, low modulus, compressibility,

* Corresponding author. E-mail: nkastor@gmail.com

and ability to easily buckle – is foam. By virtue of these properties, slots, cutouts, and long bending structures may not be needed to achieve large deformations.

Foam is particularly interesting as a structural component because it can be made from a wide variety of materials with different stiffnesses and extensibility that are otherwise solid. When made into foam, these materials change their mechanical properties dramatically, typically becoming much more compressible.[9–12] For example, a foam robot could change its shape dramatically, move through narrow spaces or holes, and then reform into its original shape without active inflation. Because foam is structurally soft and light, it creates low forces on its environment. For a similar reason, foam robots can be deformed using low-force actuators. These two features make foam robot interaction with the environment safe. Indeed, one definition of a soft robot is that, during normal operation, it will deform in response to applied forces rather than deform the environment.[13]

Specific applications that can take advantage of compressible foams include tasks that require a light touch such as fruit picking,[14–16] patient care,[17] and inspection of fragile structures.[18] Open-cell foam can be compressed for small-volume packing of robots during transport, and its resting shape is not affected by vacuum, making it suitable for applications such as inspection of a delicate antenna on the exterior of a vessel in space. Foam robots could be used for autonomous harvesting of strawberries without crushing them, or moving a person who cannot move on their own. Conventional (hard) robots are not suited for applications such as these because of the tendency of hard components to damage softer and more fragile structures.[13,19] Moreover, the field of "soft robotics" presumes that the interaction between conventional robots and fragile things, like griping lightbulbs or fruit, is a challenging problem that can be simplified by using soft and compliant materials and mechanisms.[1,2,5,20,21]

There is currently very little published knowledge about how to build and operate this type of robot. By using commonly available items (e.g., polyurethane foam, monofilament nylon cables, DC motors) and well-understood manufacturing techniques (e.g., sewing, casting, punching) we demonstrate how to rapidly produce a low-cost soft foam robot. With an underlying aim of providing a set of tools for experimentally exploring the performance and design of soft robots, we present a method that attempts to minimize components such as fasteners, or other "hard" connections, and does not require complex over-molding techniques. Furthermore, the manufacturing method is less expensive and faster than 3D printing or other rapid prototyping methods. For the cost (>$400) of a similar-sized (1.6 liter) elastomer robot printed with UV-cured resin in several hours, we can cast about 130 robots out of polyurethane foam in 30 min per mold.

Previous work on foam related to robotics focused either on the use of foam for padding and soft skin on otherwise "hard" robots,[22–33] or selected structural elements made of rigid foam in cases where buoyancy or weight were particularly important,[34–40] or soft foam robotic components such as joints, feet, or grippers.[12,22,34,41–54] However, we are aware of only four examples of systems made entirely from soft foam that move due to automated actuation. We consider these to be the only previous examples of soft foam robots.

The first is Roillo, described by the Robotics Institute at Carnegie Melon in 2006.[55] Roillo's body was completely made of soft foam, driven by motor tendons, and could move with many degrees of freedom. It was designed to be a social platform for investigating the design of nonverbal behaviors in robots, particularly for experiments on motion and gesturing for communication with children. This is an excellent example of the use of polymer foam in robotics. The authors reported that the robust foam body design facilitated human–machine interaction because it avoided damage and did not hurt the children that played with it. While the robot exhibited the features of soft foam robots and was extremely safe around humans, this machine did not locomote, as it was fixed to a table.

A second example of a soft foam robot was developed by the Creative Machines Lab at Columbia University.[10,11] This system was arranged from blocks of open- and closed-cell foam, arranged by an evolutionary algorithm to produce forward-stepping locomotion due to changes in the volume of individual blocks produced by pressure changes in an environmental chamber. The work was primarily aimed at developing and demonstrating automated evolutionary algorithms for model-based design of soft robots. The best example achieved 0.4% of a body length per second of forward locomotion speed, but could not operate outside of a pressure chamber.

The third and fourth examples of soft foam robots came from previous works by our group (Soft Material Robotics) at Tufts University. InchBot-III was built of foamed silicone and driven by shape memory alloy (SMA) actuators. This system was described in 2012.[4] InchBot-III could locomote

https://doi.org/10.1017/S0263574719000481

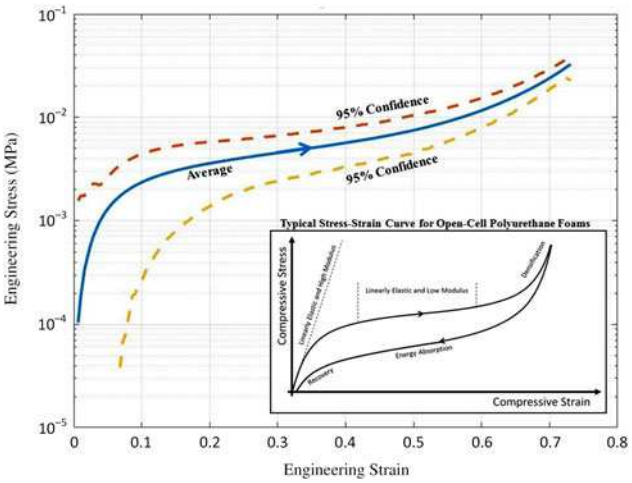

Fig. 1. Results of compression testing on polyurethane foam used in this process. The middle curve is the average of six strain rates (2, 4, 8, 16, 32, and 64 mm/min) at 30 samples each. The upper and lower bounds are 95% confidence intervals on all 180 trials. The inset compares a typical quasi-static stress–strain curve for open-cell viscoelastic polymer foams.[73–78] Hysteresis is shown in the inset for reference, but is not measured and is not part of the test data. It is possible that hysteresis effects will contribute to robot performance and should be kept in mind when designing any deformable component undergoing large strains. Designing for strains below ~50% should maintain stresses well below the densification region, minimizing hysteresis effects.

using differential friction. Published results did not quantify the motion speed. More recently, in 2017, in a close parallel to the work described here, members of our group at Tufts described a caterpillar-inspired soft robot, SquMA bot, with an open-cell polyurethane foam body driven by three-motor tendon actuators.[56] The two ends of the foam body were capped with hard ABS caps, which the actuators pulled on to produce inching locomotion. Locomotion was made possible by differential friction between the two end caps with a unidirectional roller on the bottom of each cap that only rolls forward. The robot could travel at 5.2% of a body length per second. This robot was built using a manufacturing process similar to that described in this paper.

The manufacturing method described in this work allows a robot that is molded entirely from soft open-cell polyurethane foam to be produced, with no hard end caps, and is driven by two-motor tendon actuators. The example robot can locomote at 4.3% of a body length per second, tethered to a battery and controller, on flat, smooth surfaces. Thus, we claim that, to the best of our knowledge, this work and the similar foam robot from our group[56] are the first demonstrations of soft open-cell foam robots capable of terrestrial locomotion.

Thus, the paper's main goal is to fully describe the manufacturing method used to produce this type of soft foam robot, and to delineate some of the important design decisions. We hope this method will be generally useful to the soft robotics community, and we encourage further exploration of foam robots built using this method.

2. Material Selection

Using polyurethane foam serves a few important purposes:

1) *Large elastic deformations*: The porous, open-cell nature of the material allows large deformations with little to no permanent deformation set. This allows for the exploration of interesting modes of deformation for a robot that would otherwise be difficult to create. If we were to design a mechanism that underwent complex and large deformations, it would be necessary to add many joints, with multiple degrees of freedom in each, and many members connecting them. We see this in robot design techniques such as tensegrity,[57–63] origami and kirigami,[64–69] and modular systems,[70–72] which are also very interesting. As an alternative, soft polymer foams allow for more continuum-like behavior.
2) *High strain-to-stress ratio*: Polyurethane foam is highly compressible and can change its volume followed by significant recovery facilitating shape-morphing behaviors. Figure 1 depicts the material response of testing the foam used in this process. This curve is the average of 30

https://doi.org/10.1017/S0263574719000481

samples (25 × 25 mm cylinders) tested in compression through six strain rates (2, 4, 8, 16, 32, and 64 mm/min). The upper and lower bounds show 95% confidence intervals for the whole set of data. When the material is compressed, and the air is squeezed out, the structure undergoes large linearly elastic deformation with low modulus. In the linearly elastic and low-modulus region, the robot can undergo large displacements without requiring significant power, thereby utilizing smaller and lighter motors than ones used in non-compressible robots. The return path when unloaded generally shows some hysteresis; however, this does not impact robot performance significantly. The low modulus and large deformations of the material, when used in a motor tendon–actuated robot, minimizes power consumption, even with large deformations, and allows for the use of smaller and lighter motors.

3) *Light weight*: Using the foamed form of a synthetic polymer lowers its density <1 g/cc. A lighter foam body allows faster motion and less work for motors to translate the robot. The light weight may, however, contribute to instabilities. One possible solution is to operate the robot by deforming it into static configurations as described in the example in Sections 4.4 and 6. Future work toward controlling this platform is invited and will result in stable behaviors, such as locomotion gaits. Another option to improve stability is to strategically place "heavy" internal components so that their centers of mass are close to the surface that the robot may come into contact with. In the examples presented later in this work, the motors are placed at the ends of the robot and near the ground. This creates preferred deformation in the middle of the robot and keeps its center of gravity low.
4) *A note on open-cell foams*: While polyurethane presents a wide range of mechanical properties, it is not the only material possible for this application. It is, however, readily foam-forming when created using a condensation reaction of di-isocyanates and polyols. Because polyurethane foams do present a safety hazard, due to the presence of di-isocyanate, and some of the additional small molecules in the reactive compound may be a health hazard, one may choose to substitute polyurethane with a different elastomer (e.g., foamed latex, foamed thermoplastic elastomers). However, it is important to note that many of the benefits described are only achievable with open-cell foams. Closed-cell foams do not permit the gas trapped in the cells to escape freely and thus are limited in their ability to deform to large extents. But they allow for significant spring-back of the structure and are still more compressible than the bulk, as the gas trapped inside the cells is compressible. This may be useful in other applications.

3. Actuator Selection

Many soft robots are pneumatically actuated,[79] which requires them to be built from air-tight elastic materials operating in tension.[7,80,81] Other soft devices are actuated by active materials such as SMAs[82,83] and electroactive polymers[84] that do not need to inflate and can be constructed from a variety of deformable materials and composites. Despite the versatility of active materials, they have not gained wide acceptance in robot applications because of limitations in performance, durability, or ease of control.[85] Some of the limitations of pneumatic and active material actuators can be overcome using tendon systems coupled to electric motors. Although primarily used in fixed-base manipulators,[86,87] some tendon-driven soft mobile robots have been developed.[8] In addition to their superior mechanical performance, a major advantage of motor tendons is that they can be attached to almost any material. Here we report on the design, fabrication, and testing of a method of producing (design, manufacturing, and testing) motor tendon robots fabricated using polymer foams. These robots can serve as platforms for exploring locomotion strategies, ground interaction dynamics, and control algorithms for soft compressible robots.

Motor tendon actuators apply a compressive load to the foam, creating the desired bending and buckling behaviors. Foams are not particularly strong in tension and collapse and buckle when compressed. Tension-based actuation (e.g., muscle and tendon) is the primary mechanism for producing animal movements, and the development of whole-body tension is used by some soft animals and robots as a strategy for crawling without compromising deformability.[4,8,88–91] Similarly, tension is used to actuate the robot and compress the foam. It should be noted that tension can be driven by a variety of other actuators (e.g., SMAs, electroactive polymers, artificial or lab-grown muscle) and not just by electric motors. We have chosen motor tendons because they provide powerful, fast, and efficient actuation to obtain the desired behaviors.

https://doi.org/10.1017/S0263574719000481

4. General Design Rules

As designers of this type of soft robot, we should make sure to preserve, and leverage, the properties of the foam and to create interesting and useful devices. Ensuring that the body of the robot remains compressible and easily deformable is paramount to the notion of a soft robot, and thus it is important to carefully consider the addition of any stiff, or heavy, components (e.g., printed circuit boards [PCBs], motors). Combining a foam body with motor tendon actuators allows the use of a single or a few motors. However, design still requires attention to certain important concepts to ensure successful implementation, as described in subsequent sections.

4.1. Robot size and shape

In the example presented in Section 6, the morphology of the robot is abstract, but a specific application may demand particular size and shape. Nevertheless, it is important to remember that the foam is compressible, and the shape of the body will deform easily, conforming to the environment. Therefore, the shape of the robot is not critical, beyond where the components will be located in relation to each other. The space between the components is effectively filled with foam, and the stiffness and mass of those components will dominate the system. In order to design a robust system there must be enough foam material between components so that the robot can assume the shape required. For example, if the focus is on locomotion, as presented in the following example, the size of the foam body would be chosen to produce a certain stride length. If this particular robot needed to fit through an opening, then perhaps the corners should be chamfered and the body tapered to ease the transition; however, as the compressible body deforms, the orientation of hard components will be most important to minimize interference with the soft structure.

4.2. Component placement

The components embedded in the foam body affect the performance of the robot. When considering an application, the designer should keep in mind that the use of certain hard or inflexible components is unavoidable. However, these components can be used to our advantage to make a better-performing robot. For example, heavy components, such as the motors, can be used as ballast to control the shape of the robot or as weight for friction manipulation. Another example is that stiff circuit boards will interfere with the folding and compressing of the soft body. Therefore, care must be taken when placing stiff components so that their orientation is appropriate to maintain the desired configurations and shapes.

4.3. Actuation speed

Actuation speed is of particular interest for soft foam robots because they exhibit different behaviors depending on how quickly they are actuated, much like other viscoelastic synthetic materials. As expressed in Section 2, there is a mild strain rate dependence in material response. Also, at higher speeds, the effect of robot body and component inertia causes dynamic motions, such as leaping forward rather than stepping. These two ideas can be a benefit or a hindrance depending on the design intent, yet moving quickly is not necessarily the best application for soft robots. Indeed, energy is absorbed by the soft and compressible foam material, making fast motions difficult. It may be that the best niche for soft foam robots is with slow, quasi-static motions to form configurations.[92] In this way, our robot can assume a particular shape in order to accomplish a task. For example, a crawling gait in a terrestrial robot could be created by alternating between flat and folded configurations.

4.4. Tendon routing

Different configurations are created by routing the tendon of our motor tendon actuator. There are three ways that the tendon can interact with the foam: (1) at the actuator (in this case it is an electric DC motor); (2) the anchor of the other end of the tendon; and (3) where we would like the tendon to pass through the foam. Figure 2 illustrates some possible configurations with different combinations of motor, anchor, and pass-through.

Two primitive configurations are created with one-motor tendon actuator and a slab of foam depending on the orientation. Figure 2(a) shows a concave up arc when the tendon runs across the top side of the slab, and (b) shows a concave down arc when the tendon is routed along the bottom. With these two simple shapes the designer can imagine numerous applications involving crawling

https://doi.org/10.1017/S0263574719000481

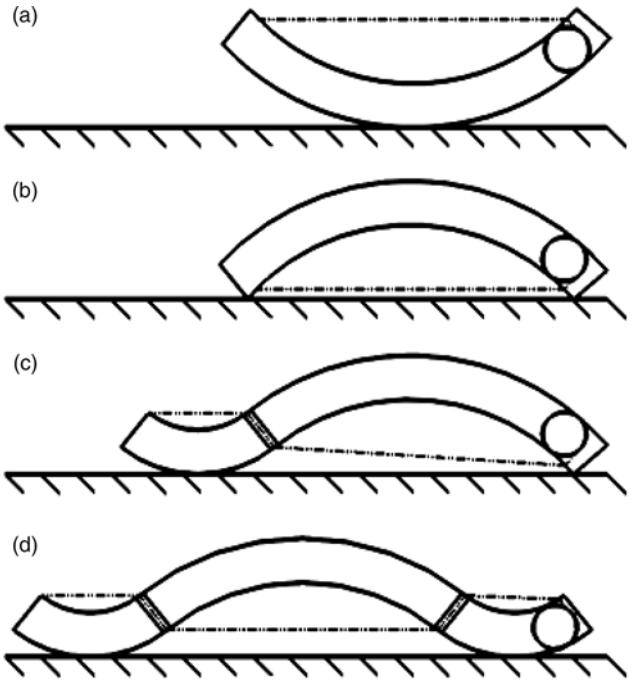

Fig. 2. Examples of deformed shapes with different tendon routing. The motor is shown as a circle within the foam body. (a) Concave up shape with the tendon along the top of the foam. (b) Concave down shape with the tendon along the bottom. (c) When A and B are combined, an S-shape is created. (d) Two S-shapes combined.

and grasping. Combining shapes A and B would result in more complex configurations such as those presented in Fig. 2(c, d).

The large plateau region exhibited by open-cell foams (see Fig. 1) makes the foam body easy to deform, and thus the dimensions of configurations shown (Fig. 2) are dependent on the distance between the three interaction methods. For example, a taller arc in Fig. 2(b) could be formed by a longer distance between the anchor and motor. In Fig. 2(c), we control the S-shape with the placement of the tendon pass-through. A shorter distance between pass-through and anchor makes the concave up portion small and the concave down portion large. In a similar fashion, the robot can be deformed to create 2D or 3D configurations by altering the tendon path out of plane.

When the motor spools the tendon, the anchor point and the motor are drawn toward each other. As a result, any foam between points of interaction with the tendon is buckled and pushed away. Keeping this in mind, we can imagine the robot as behaving like line segments within the foam that shorten and lengthen as the motor spools and unspools the tendon. In the example shown in Fig. 3, the tendon length shortens pulling points 1, 2, and 3 closer together. This new configuration will buckle out of plane in the manner described in Fig. 2.

It should be noted that external tendons are used in this design method and shown in the robot examples in Section 6. External tendons limit the application environments, and a method for enclosing the tendons is required for navigation of unstructured environments. Indeed, this is a nontrivial matter. A method to embed the tendons should retain the compressible properties of the foam and not limit the desired large deformations. This said, the method presented here generates useful, and easily configurable, prototypes for exploring design space, locomotion gaits, and control methods. More advanced, and detailed, methods and techniques of production are a matter of future work using this platform.

4.5. Tendon–foam contact

The end of the tendon not attached to the motor is anchored to the foam body. In addition, at certain locations, the tendon passes through the soft foam body as shown in Figs. 2 and 3. Achieving reliable tendon–foam contact sites requires attention to three aspects: (1) Stresses on the foam by the tendon can cause the foam to tear. (2) Friction between the tendon and foam contact surfaces can be high, especially when the body is deformed and constricts the contact site. (3) The assembly method should be easy to be performed and repeated to allow for rapid reconfiguration.

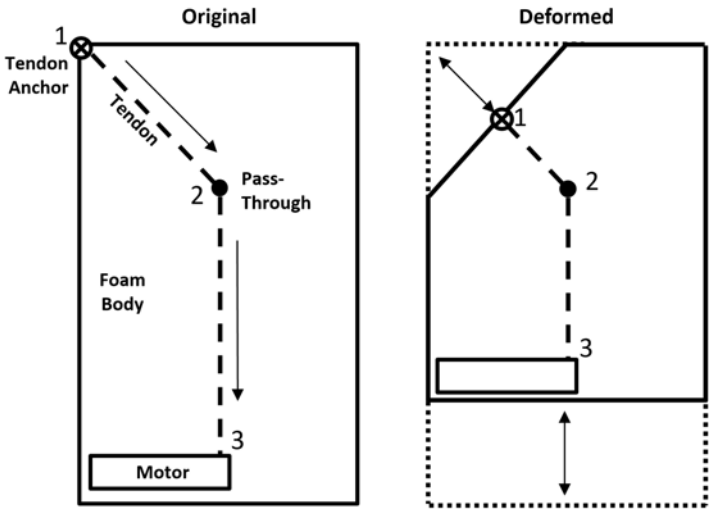

Fig. 3. Points 1, 2, and 3 are drawn together as the tendon is spooled. The system responds between points of interaction with the tendon and foam; therefore, the deformed shape is that of the out-of-plane shapes shown in Fig. 2 along the tendon path above.

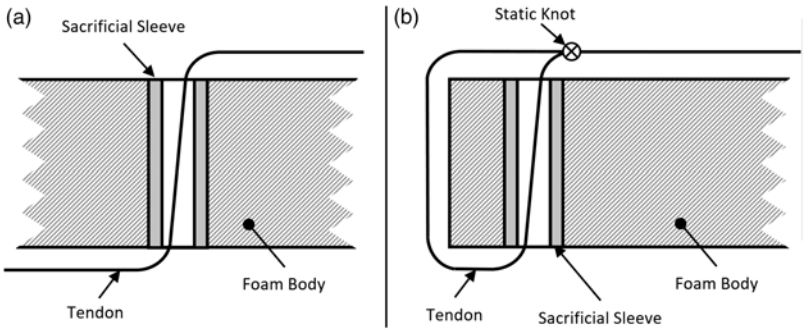

Fig. 4. A close view of the tendon–foam contact assembly at an arbitrary inflection point A and the tendon anchor B. The tendon passes through the foam body in both A and B, and a sleeve of sacrificial material is added to the hole so that the tendon does not damage the foam. As described in Section 5-J, hot melt adhesive is used to fix the sleeve to the foam. At the anchor, the tendon is routed through a hole in the foam body, looped around the outside, and tied with a static not that does not slip.

To achieve reliable sliding contacts, such as in those locations where the tendon passes through the body, a sleeve of sacrificial material (silicone tubing) is used to protect the soft foam body (Fig. 4(a)). The sleeve distributes the load of the tendon on the body and inhibits tearing of the foam. A lubricant is added to reduce the friction and allows the tendon to pass smoothly. At the anchor site, the tendon is passed through a sleeved hole and tied to itself (Fig. 4(b)). A static (non-slipping) knot is used so that the tendon loop does not constrict the assembly and cut through.

These features do not require special processes or tools, and can be implemented without special training. Implementing these features increased the longevity of the assembly from only a few gait cycles to several trials of many gait cycles each, while remaining semi-permanent to allow for reconfiguration.

4.6. Motor selection

There are three main factors that influence the selection of actuator motors: (1) foam compressibility, (2) friction along the tendon path, and (3) the mass of motor assembly. It is important to select a motor assembly that is heavier than the foam body. In this case the friction at the point below the motor will be higher than the points that do not have a heavy component above. At the same time, it is also important that the motor be strong enough to compress the foam and overcome the friction along the tendon path. Lubrication at the points where the tendon interacts with the foam body will greatly facilitate spooling; therefore, the required motor torque T is only dependent on the force required to collapse the foam structure F and the amount of tendon spooled ΔL as shown in Fig. 5.

https://doi.org/10.1017/S0263574719000481

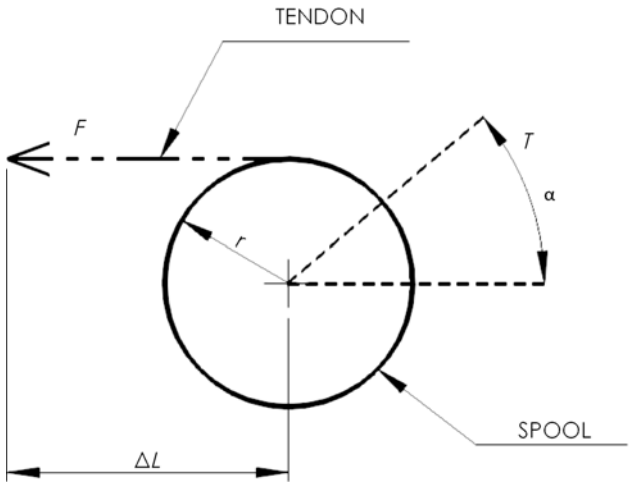

Fig. 5. Motor spool and tendon force diagram. Tendon force F is equal to the torque on the spool multiplied by spool radius r. The angle of spool rotation α is proportionate to the length of tendon spooled ΔL.

We may define the work of rotating the spool as the required torque multiplied by the angle of rotation α:

$$W_{spool} = T \cdot \alpha \tag{1}$$

and the linear work done on the tendon as:

$$W_{tendon} = F \cdot \Delta L \tag{2}$$

Work is done by the motor on the tendon to compress the foam; therefore, using (1) and (2), the required minimum motor torque is

$$T = \frac{F}{\alpha} \Delta L \tag{3}$$

Determining F, and thus a minimum T, can be done via compression testing as explained in Section 2. The parameters α and ΔL are related to the desired stride length or behavior of the robot.

4.7. Attaching "hard" components

Soft actuators and soft electronics are of great interest for future versions of this system; however, at availability is limited. As a result, designers of soft robots are required to make allowances for "hard" components such as motors and PCBs. A useful method, which we employ here for attaching components that are much harder than the foam, is suturing into cavities cut into the body. A cavity can be easily cut into the foam in any orientation using a razor. The component can then be located on the body using this cavity and sutured in place. If the sutures are tied loosely, the component does not fall off the robot, yet can float freely, minimizing interference and reducing the stiffening effect of the hard component. Cutting cavities and other features into the foam also reduce the stiffness of that section; so care must be taken to locate the feature in a place that will either benefit or not be encumbered by a decrease in stiffness.

4.8. Control

There is an extremely large set of actuator and tendon path combinations; and designing for a specific application is a complicated optimization problem that is outside the scope of this paper. In addition, computational design of control schemes requires an accurate model of the large deformation and nonlinear mechanics of the body, including time-varying structural properties and friction. This is further complicated by the challenge of modeling interaction with an often unknown and unstructured environment. Fortunately, the easily compressible nature of soft foam and its tendency to move slowly, provide substantial damping, and not damage the environment allow considerable flexibility in control schemes. We have found that repetitive gait cycles using motor position control can be intuitively designed and experimentally verified and iterated without much difficulty. These

https://doi.org/10.1017/S0263574719000481

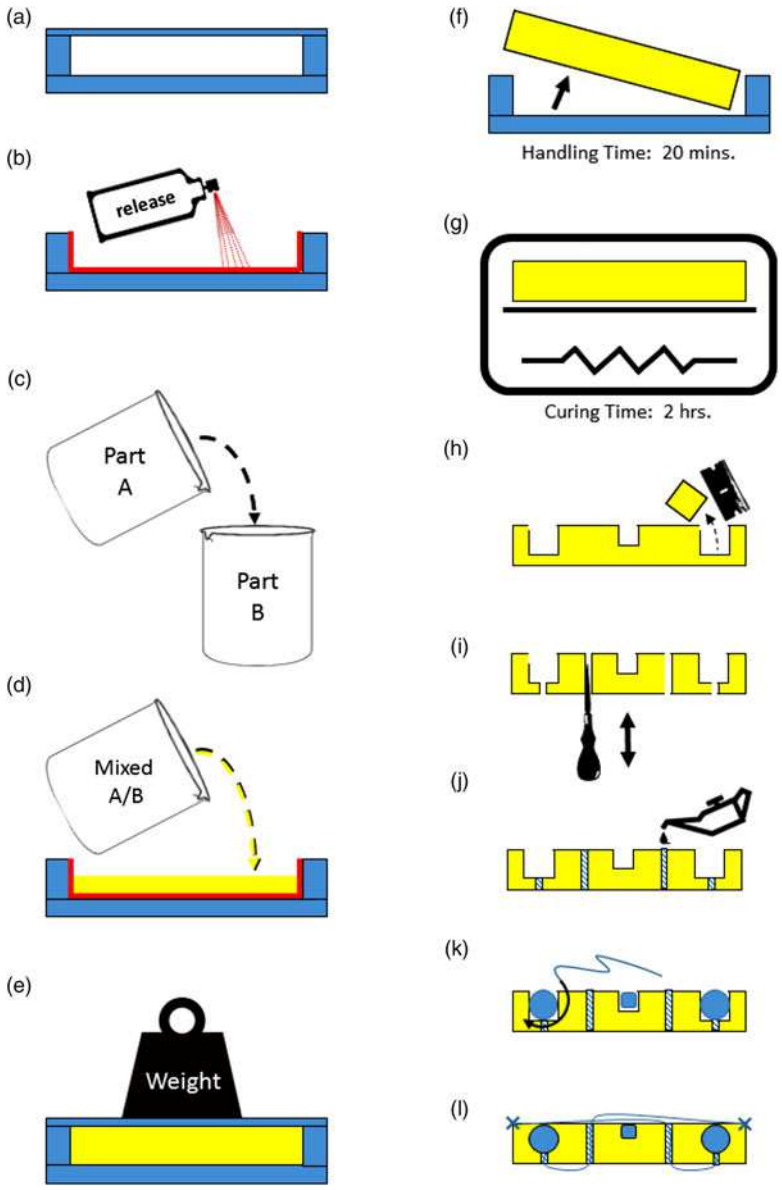

Fig. 6. The manufacturing process.

gait cycles can form a set of primitives for moving, turning, flipping, or other behaviors, as will be demonstrated in the examples in the next sections.

5. Manufacturing Method

The manufacturing process (Fig. 6) uses traditional casting techniques using self-expanding polyurethane foam for the robot body (Fig. 6). Instead of placing the components into the mold, all components are attached via suturing at the end of the process to create a functioning robot. Such amalgam of textile engineering technologies with robotic sensors and actuators is unique and has not been explored elsewhere.

A. A simple rectangular mold made of laser-cut sheets of acrylic in the size of the final foam slab is constructed. The lid is removable and secured by weight only. By this way, venting of air during foaming will occur through the gap between the top and cavity.
B. The mold and lid are coated with a compatible release agent (Miller-Stephenson MS-143XD PTFE) to facilitate the removal of foam slab. A release agent is always required when molding; therefore, some release agent will be on the surface of the robot. Any change in the surface

chemistry will affect the coefficient of friction and thus the locomotion of the robot. This can be mitigated by cleaning the surface.

C. Polyurethane foam (BJB Enterprises TC-274 Polysoft 2) is mixed from two parts, A and B, diol and di-isocyanate (along with other small molecules). The urethane reaction proceeds to release gas and water, thus forming open-cell pores that make the foam. The materials are measured by volume to achieve the final desired part volume.

$$V_{\text{final}} = V_{\text{initial}} \cdot C_{\text{expansion}} \tag{4}$$

$$V_{\text{initial}} = V_{\text{part A}} + V_{\text{part B}} \tag{5}$$

$$V_{\text{part A}} = R_{\text{volume}} \cdot V_{\text{part B}} \tag{6}$$

where $C_{\text{expansion}}$ and R_{volume} depend on the material and are provided by the manufacturer. V_{final} is the volume of cured material used in the robot body, and $V_{\text{part } i}$ are the measured volume amounts of the two (typically two) reactants. It is important to premix both parts separately, before combining, in order to ensure homogeneity of the polymer chains. The pot life for the material used here is short ($\sim$10 s after mixing); so parts A and B should be added quickly and stirred with a "jiffy-mixer" until fully mixed. The mixer should be turned slowly in order to prevent air from being entrained into the mixture, thus avoiding large voids in the final structure.

D. The mixture of A and B should be poured into the mold before foaming occurs in order to prevent local density gradients. For the same reason, the mold is rotated slowly so that the polymer coats the entire inside. The material will then foam evenly and reduce the number of internal phase boundaries.

E. The lid of the mold is placed on top and a 5 kg weight is added to prevent the foam from pushing the mold open.

F. After the handling time of 20 min is reached, the mold can be opened and the slab removed.

G. Final post-curing is conducted in a convection oven with no direct radiation at 40°C for 2 h or 12 h at >20°C.

H. In this step the desired final geometry of the robot is cut with a razor. Flash is removed by chamfering the edges. The design described in this paper calls for two-motor tendon assemblies to be installed as actuators. Blind slots are cut for the motors and other components.

I. An awl is used to punch holes through the slab for the tendon path. The robots described here have locations where the tendons pass through the body, which produces a particular motion. It is possible to quickly produce different motions by punching holes in different locations and moving the tendon path.

J. Nylon monofilament tendons (South Bend M148, 8 lb fishing line) are used to pull on the structure of the slab. Since the tendon is thin (300 μm diameter), and nylon is hard in comparison to polyurethane, the tendon can cut into the polyurethane foam during actuation. Therefore, silicone tubing (500 μm wall, 2 mm O.D.) is used to line the holes where the tendon passes to reduce wear. A very small amount of hot melt adhesive is used to tack the tubing in place so it does not slide out of the hole. During actuation there is significant friction in the tendon path as the structure collapses and folds. This causes undesirable effects, such as increased wear and increased motor load. A thin film of lubricant (3-in-1 multipurpose oil) is added to alleviate these problems by applying a few drops to the inlet of the tubing.

K. At this point, motors and components can be placed in the cut-out locations. All the components are sutured in place using a curved sewing needle and the same nylon tendon. Suturing allows the components to "float" in place and reduce coupling with the foam structure. If an adhesive were to be used, then there would be significant stress applied to the interface between the component and the foam, resulting in failure. The sutured components minimally interact with the foam, increasing compliance and a variety of deformed shapes.

L. Now that the components are affixed to the structure, the tendons can be routed from the motor spools to their respective anchor points. The designs shown in this paper have the tendons emerging from the bottom of the slab, passing through one hole, and anchored to the opposite corner. A hole is punched through the slab near the corner and a length of silicone tubing is placed. The tendon passes through this tube and is looped around the corner and knotted to itself. When the motor is actuated the tendon is spooled and pulls on this anchor point, thus collapsing the robot.

https://doi.org/10.1017/S0263574719000481

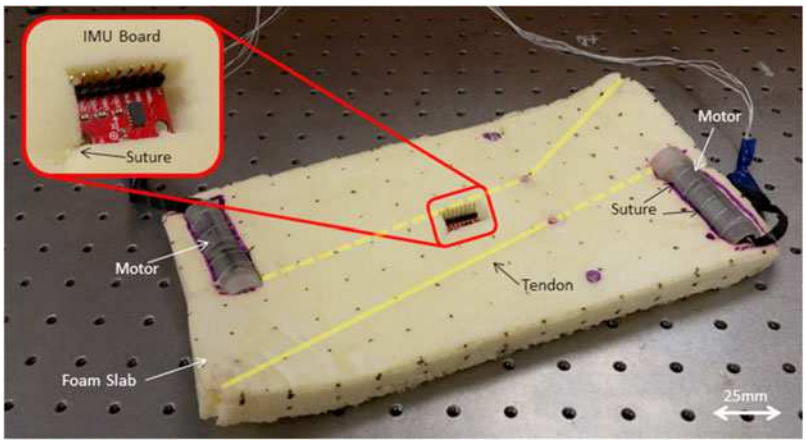

Fig. 7. The robot pictured is a slab of polyurethane open-cell foam that is actuated with two-motor tendon actuators. The tendon path is highlighted in yellow where solid lines are on the top surface and dashed lines are hidden along the bottom surface. The robot is capable of crawling, turning, and complex shape changing despite its simple design. Components such as inertial measurement units (IMUs) and motors are attached by suturing with monofilament nylon sutures as shown in the close-up view. The same monofilament line is used to drive deformations in the robot by means of motor tendon actuators.

6. Robot Example

Using this manufacturing method and design methodology, we demonstrate an example of a soft and compressible terrestrial robot that, even with a simple geometry (Fig. 7), exhibits complex behavior with only two actuators. The body of the robot is a $300 \times 150 \times 25$ mm rectangular slab of compressible open-cell foam that is contorted by two-motor tendon actuators. The motors, tendon paths, and anchor points are arranged as shown in Fig. 7. The motor placement, tendon paths, and anchor points are chosen based on the design rules above and with attention to how ground reactions and differential friction affect locomotion.[90,93] For example, as seen in Fig. 7, the motors are placed at the ends so that their weight will produce the most friction while crawling. The most effective gaits are then determined experimentally.

The motor tendon assembly is constructed of a Maxon DC 237011 motor press fit into a 3D-printed housing. This is a 14-mm-diameter, 25.5-mm-long brushed DC motor with a planetary gearhead at a 231:1 reduction ratio and a maximum output torque of 0.2 N·m. The motor housing is manufactured from simultaneous printing of UV-cured rigid polymer (Stratasys VeroClear RGD810) to provide structure, and a soft polymer exterior (Stratasys TangoPlus FLX930) for improved friction with the sutures. To create the interference fit, motor housings are placed in an oven at 60°C to expand, and the motors are pressed in and allowed to cool to room temperature. A spool is attached by the same interference fit method to the motor shaft and is used to spool the tendon as the robot is actuated. Tendon lines are attached to the spool by knotting and securing with epoxy. The tendon material used here is monofilament nylon; however, any material that is flexible and does not noticeably stretch would work. When the motor is inserted into the appropriate cavity in the robot body, it is sutured in place, with the same tendon line, using a standard curved leather sewing needle. The sutures are pulled tight to grip the soft exterior of the motor housing. With enough windings of the suture there is sufficient friction to hold the housing in place and transfer the majority of energy in the spinning armature to spool the tendon and collapse the foam structure.

Tendons are anchored to the opposite corners from their origin at the motor. Along their path, the tendons pass through the body at certain points (as shown in Fig. 8) to collapse the foam structure when actuated. The majority of the tendon does not interact with the body of the robot; however, where the tendon passes through the body, a force and moment are applied at that point. As seen in Fig. 9, when the actuator assembly shortens the tendon, the points of interaction are drawn toward the motor, compressing and bending the foam along the tendon path to change the shape of the robot. As a result, contact area between the ground and robot changes shape and size, thus creating differential friction and propelling the robot. By rearranging the tendon path, a different folding, compressing, and locomotion regime can be achieved, which would result in an alternate gait and shape change.

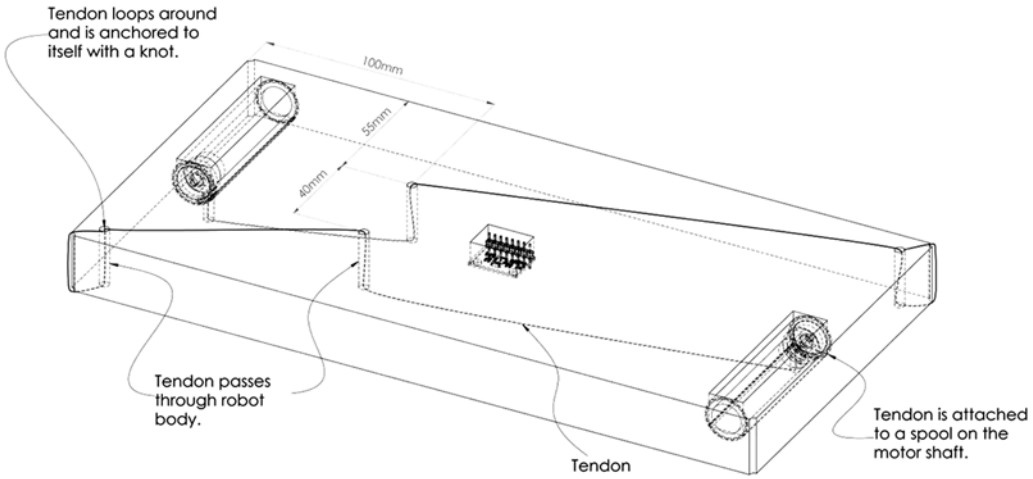

Fig. 8. A schematic drawing of one possible configuration of the foam robot. In this iteration we have two-motor tendon actuators with tendons routed through the first third of the body of the robot. The ends of the tendons are anchored at the corners, as shown, by passing through the body, looping around, and tying back to the tendon with a static knot that does not slip.

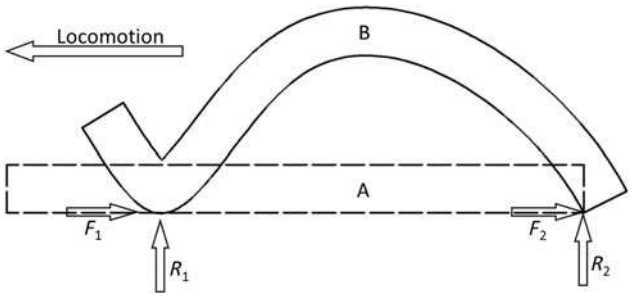

Fig. 9. The original shape of the robot is shown as A. When the shape is deformed to B, the normal force R and surface area in contact with the ground change and create differential friction elements. The robot will move when the new shape B is oscillated and the friction forces F change with time.

A benefit of this simple design is that multiple configurations can be created by punching new holes and re-routing the tendons.

Simple changes in tendon routing have dramatic effects on the robot's behavior. For example, 2D locomotion (i.e., turning) is exhibited when the center of mass is displaced to a position that is out of plane from the motion shown in Fig. 9. When the robot is deformed in two orthogonal planes (horizontal and vertical), the points at which the robot interacts with the ground are no longer in line, bending the robot body and revealing a turning gait. Fig. 10 shows one possible configuration that would create this scenario. Moving the tendon pass-through closer to the motor, past the centerline, lengthens the angled portion, creating a bent deformed configuration that would cause the robot to turn.

Interesting behaviors emerge when the length of tendon spooled is varied. Forward crawling is exhibited when the tendon is spooled, so that the robot oscillates between the configurations shown in Fig. 9. Spooling the tendon further, as shown in Fig. 11, would result in a different behavior such as end-over-end flipping. The crawling gait has two points of contact with the ground and the center of mass between them. Spooling the tendon more moves the center of mass even further forward so that the robot falls over, and on release of the tendon tension, the robot unfolds to lay flat and upside down.

In the same manner as the actuators, sensors can be attached to the robot body as shown in Fig. 7. Any small PCB or flex circuit with a sensor, such as the inertial measurement unit (Sparkfun MMA7361) shown, may be sewn onto the foam body. The holes that are traditionally designed into PCBs for fastening using screws are a useful anchor points for sewing. If the attachment points are

https://doi.org/10.1017/S0263574719000481

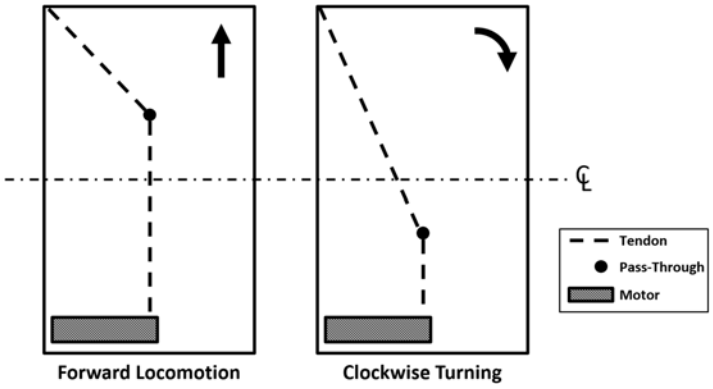

Fig. 10. Changes in location of the hole where the tendon passes through the body resulting in different locomotion behaviors. In this example, moving the pass-through back toward the motor lengthens the angled portion of the tendon, creating a bent deformed configuration, thus resulting in a turning gait.

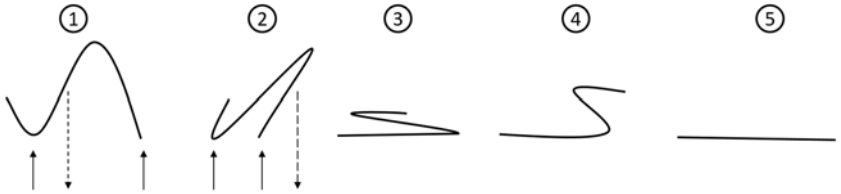

Fig. 11. End-over-end flipping behavior. (1) Deformed configuration with two ground contact points (solid arrows) on either side of the center of mass (dotted arrow). (2) The tendon is spooled further and the center of mass is now moved past the contact points. (3) The robot falls to one side. (4) Tendon tension is released. (5) The body of the robot is now flat and upside down.

few, and thus the PCB not over-constrained, the PCB "floats" with respect to the robot body and does not interfere with locomotion. This is a step toward total autonomy of the robot.

6.1. Experiment

The robot is tested on an optics table where the surface is ground steel with 1-inch-spaced holes for mounting optic components. The robot is tethered to an off-board power supply and electronics to focus the project on the deformation of foam body and manufacturing methods, and less on the interaction of components. Motor voltage is set to constant 15 V and the motors draw <1 A during actuation. Current to the motors is controlled via Toshiba TA8428K motor drivers and operated by an embedded microcontroller script. An open-loop control method is employed where the motor forward and backward spooling is timed and synchronized manually to produce locomotion gaits.

6.2. Performance

With only two actuators and arbitrary tendon placement, the robot is capable of dramatic shape change (Fig. 12). The robot exhibits forward crawling (Fig. 12(a)), in-place turning (Fig. 12(b)), and end-over-end flipping (Fig. 12(c)) behaviors by altering the normal force over the surface area in contact with the ground via shape and volume change. For example, the robot flips when the robot folds itself in half, decreasing contact area to 17% and moving the center of mass forward past this contact area.

Locomotion depends on differential friction and, thus, on normal force and friction coefficient (contact with surface asperities and adhesion) with the substrate. The body must be contorted into a shape that has mass distributed unevenly over contact patches. Orienting these contact patches appropriately yields different types of motion, such as crawling and turning. For example, some configurations arrange the mass of the robot so that there is more weight over the front contact area than the rear contact area (Figs. 8 and 11(a)). These result in the rear of the robot being pulled to the front during actuation. When the motor is run backward, the spool unwinds and the robot lays flat. As tension is released, the body changes shape again and there is enough friction on the rear

https://doi.org/10.1017/S0263574719000481

Fig. 12. Left: The robot demonstrating a crawling gait. This gait produces a forward locomotion speed of ∼13 mm/s. Center: The robot demonstrating a turning gait. Each motion of this configuration produces ∼18° of rotation. Right: The robot demonstrating a flipping behavior.

surface to overcome the friction on the front, propelling the robot forward. Forward crawling speed is ∼13 mm/s on the steel surface of the optics table shown with the maximum current drawn being <500 mA at 15 V.

To make the robot turn, a contact area is formed on one side by rearranging the mass, allowing the body to pivot about that patch. By actuating the opposite corner, the robot turns ∼9°/s (Fig. 12(b).

The flipping behavior (Fig. 12(c)) occurs when the robot folds itself into an over-center configuration where the center of mass is now beyond the front motor. When the motors unspool, the robot flips over and is now upside down.

To extend beyond these quasi-static ideas, the notion of differential friction and tendon placement can become more complex when the robot is actuated at different rates. Open-cell foam deformation response is strain rate–dependent, and in addition, inertial effects become important at higher speeds. Therefore, when the tendons are wound quickly, we see a variation in behavior depending on the rate. Additionally, how the tendon is routed and where it interacts with the body of the robot can change the deformed shapes. When these two variables are combined, a large number of gaits can be produced from a small number of actuators.

7. Conclusion

The design and manufacturing method described in this paper allows for rapid and low-cost production of foam robots. Robots can be built at a rate of ∼30 min per mold, at under $3 per robot for the structural foam, and in a large variety of shapes given the flexibility afforded by the molding and suturing process.

Many different gaits and movements are possible with different body shapes, actuator positions, and tendon routing. In this work we demonstrated forward crawling at 13 mm/s (4.3% of a body

https://doi.org/10.1017/S0263574719000481

length per second), turning at 9°/s, and end-over-end flipping, using two-motor tendon actuators and a simple rectangular shape. Future work using this manufacturing and design method can explore the immense design space for these robots, which includes body shape, tendon paths, motor placement, and strain rate. Soft foam molding with sutured motors and motor tendon actuators offers a promising method for the production of many unique prototypes for future research in materials, controls, and system modeling of soft robots.

Polyurethane open-cell foam and sutured components, in particular, demonstrate many of the desirable characteristics of soft robots in that they: (1) conform their bodies to the environment, rather than deforming the environment; (2) change shape in multiple dimensions; and (3) exhibit complex behaviors, such as gaits for locomotion. These characteristics offer many opportunities for automatic and adaptive control strategies, such as those seen in ref. [90].

Further work is ongoing for achieving a fully autonomous motor tendon–actuated soft robot using the techniques described in this work. We are particularly interested in exploring dynamic weight redistribution to achieve robust locomotion by controlling where the system "sticks" and "slips" on the surface. Incorporation of control electronics and a light-weight power source appear achievable. Challenges remain in system modeling and gait optimization. In addition, more work is needed to consider the many novel application areas best addressed by soft robots.

Acknowledgment

Special thanks to Camille–Louise Mbayo for collecting the test data from materials. This research was supported in part by the National Science Foundation (NSF) grant IGERT-1144591. 3D printing was made possible by an NSF award DBI-1126382.

References

1. H. Abidi and M. Cianchetti, "On intrinsic safety of soft robots," *Front. Robot. AI* **4**, 5 (2017).
2. C. Laschi, B. Mazzolai and M. Cianchetti, "Soft robotics: Technologies and systems pushing the boundaries of robot abilities," *Sci. Robot*. **1**(1), eaah3690 (2016).
3. S. Kim, C. Laschi and B. Trimmer, "Soft robotics: A bioinspired evolution in robotics," *Trend Biotechnol*. **31**(5), 287–294 (2013).
4. B. A. Trimmer, H.-T. Lin, A. L. Baryshyan, G. G. Leisk and D. L. Kaplan, "Towards a biomorphic soft robot: Design constraints and solutions," *2012 4th IEEE RAS & EMBS International Conference on Biomedical Robotics and Biomechatronics (BioRob)*, Rome, Italy (IEEE, 2012).
5. D. Rus and M. T. Tolley, "Design, fabrication and control of soft robots," *Nature* **521**(7553), 467–475 (2015).
6. M. Calisti, G. Picardi and C. Laschi, "Fundamentals of soft robot locomotion," *J. Royal Soc. Interface* **14**(130), 20170101 (2017).
7. M. T. Tolley, R. F. Shepherd, B. Mosadegh, K. C. Galloway, M. Wehner, M. Karpelson, R. J. Wood and G. M. Whitesides, "A resilient, untethered soft robot." *Soft Robot*. **1**(3), 213–223 (2014).
8. T. Umedachi, V. Vikas and B. A. Trimmer, "Softworms: The design and control of non-pneumatic, 3D-printed, deformable robots," *Bioinspir. Biomim*. **11**(2), 025001 (2016).
9. N. Cheng, G. Ishigami, S. Hawthorne, H. Chen, M. Hansen, M. Telleria, R. Playter and K. Iagnemma, "Design and analysis of a soft mobile robot composed of multiple thermally activated joints driven by a single actuator," *2010 IEEE International Conference on Robotics and Automation (ICRA)*, Anchorage, Alaska, USA (2010).
10. J. Hiller and H. Lipson, "Automatic design and manufacture of soft robots," *IEEE Trans. Robot*. **28**(2), 457–466 (2012).
11. H. Lipson, "Challenges and opportunities for design, simulation, and fabrication of soft robots," *Soft Robot*. **1**(1), 21–27 (2014).
12. B. C. Mac Murray, X. An, S. S. Robinson, I. M. van Meerbeek, K. W. O'Brien, H. Zhao and R. F. Shepherd, "Poroelastic foams for simple fabrication of complex soft robots, *Adv. Mater*. **27**(41), 6334–6340 (2015).
13. N. Kastor, V. Vikas, E. Cohen and R. D. White, "A definition of soft materials for use in the design of robots," *Soft Robot*. **4**(3), 181–182 (2017).
14. C. W. Bac, E. J. van Henten, J. Hemming and Y. Edan, "Harvesting robots for high-value crops: State-of-the-art review and challenges ahead," *J. Field Robot*. **31**(6), 888–911 (2014).
15. C. W. Bac, J. Hemming, B. A. J. van Tuijl, R. Barth, E. Wais and E. J. van Henten, "Performance evaluation of a harvesting robot for sweet pepper," *J. Field Robot*. **34**(6), 1123–1139 (2017).
16. Y. Sarig, "Robotics of fruit harvesting: A state-of-the-art review," *J. Agric. Eng. Res*. **54**(4), 265–280 (1993).
17. M. Cianchetti, C. Laschi, A. Menciassi and P. Dario, "Biomedical applications of soft robotics," *Nat. Rev. Mater*. **3**, 143–153 (2018).
18. M. R. Jahanshahi, W.-M. Shen, T. G. Mondal, M. Abdelbarr, S. F. Masri and U. A. Qidwai, "Reconfigurable swarm robots for structural health monitoring: A brief review." *Int. J. Intell. Robot. Appl*. **1**(3), 287–305 (2017).

https://doi.org/10.1017/S0263574719000481

19. A. Chen, R. Yin, L. Cao, C. Yuan, H. K. Ding and W. J. Zhang. "Soft robotics: Definition and research issues." *24th International Conference on Mechatronics and Machine Vision in Practice (M2VIP)*, Auckland, New Zealand (IEEE, 2017).
20. J. Hughes, U. Culha, F. Giardina, F. Guenther, A. Rosendo and F. Iida, "Soft manipulators and grippers: A review," *Front. Robot. AI* **3**, 69 (2016).
21. C. Majidi, "Soft robotics: A perspective—current trends and prospects for the future," *Soft Robot*. **1**(1), 5–11 (2014).
22. G. Monkman, "Robotic compliance control using memory foams," *Ind. Robot Int J*. **18**(4), 31–32 (1991).
23. J. Saldien, K. Goris, B. Verrelst, R. Van Ham, and D. Lefeber, "ANTY: The development of an intelligent huggable robot for hospitalized children." *9th International Conference on Climbing and Walking Robots and the Support Technologies for Mobile Machines*, Brussels, Belgium (2006).
24. T. Minato, Y. Yoshikawa, T. Noda, S. Ikemoto, H. Ishiguro and M. Asada, "CB2: A child robot with biomimetic body for cognitive developmental robotics," *2007 7th IEEE-RAS International Conference on Humanoid Robots*, Pittsburgh, Pennsylvania, USA (IEEE, 2007).
25. J.-H. Oh, D. Hanson, W.-S. Kim, Y. Han, J.-Y. Kim and I.-W. Park, "Design of android type humanoid robot albert HUBO," *2006 IEEE/RSJ International Conference on Intelligent Robots and Systems*, Beijing, China (IEEE, 2006).
26. L. Zeng and G. M. Bone, "Design of foam covering for robotic arms to ensure human safety," *Canadian Conference on Electrical and Computer Engineering, CCECE 2008*, Ontario, Canada (IEEE, 2008).
27. M. Hayashi, T. Yoshikai and M. Inaba, "Development of a humanoid with distributed deformation sense with full-body soft plastic foam cover as flesh of a robot," *J. Robot. Soc. Japan* **26**(8), 925–931 (2008).
28. T. Minato, M. Shimada, H. Ishiguro and S. Itakura, "Development of an Android Robot for Studying Human–Robot Interaction," *17th International Conference on Industrial, Engineering and Other Applications of Applied Intelligent Systems*, Ottawa, Canada (Springer, 2004).
29. J. Saldien, K. Goris, B. Vanderborght, J. Vanderfaeillie and D. Lefeber, "Expressing emotions with the social robot probo," *Int J. Soc. Robot*. **2**(4), 377–389 (2010).
30. R. Bischoff and V. Graefe, "Hermes—an intelligent humanoid robot designed and tested for dependability," *2002 International Symposium on Experimental Robotics*, Sant'Angelo d'Ischia, Italy (Springer, 2003) pp. 64–74.
31. K. Goris, J. Saldien, I. Vanderniepen and D. Lefeber, "The huggable robot probo, a multi-disciplinary research platform," *International Conference on Research and Education in Robotics (EUROBOT)*, Heidelberg, Germany (Springer, 2008).
32. Y. Ohmura and Y. Kuniyoshi, "Humanoid robot which can lift a 30 kg box by whole body contact and tactile feedback," *IEEE/RSJ International Conference on Intelligent Robots and Systems, IROS 2007*, San Diego, CA, USA (IEEE, 2007).
33. Y. Yamada, Y. Hirasawa, S. Huang, Y. Umetani and K. Suita, "Human–robot contact in the safeguarding space," *IEEE/ASME Trans. Mech.* **2**(4), 230–236 (1997).
34. K. Hirata, T. Takimoto and K. Tamura. "Study on turning performance of a fish robot," *First International Symposium on Aqua Bio-Mechanisms*, Honolulu, Hawaii (2000).
35. K. Takagi, M. Yamamura, Z.-W. Luo, M. Onishi, S. Hirano, K. Asaka and Y. Hayakawa, "Development of a rajiform swimming robot using ionic polymer artificial muscles," *2006 IEEE/RSJ International Conference on Intelligent Robots and Systems*, Beijing, China (IEEE, 2006).
36. R. K. Katzschmann, A. D. Marchese and D. Rus, "*Hydraulic autonomous soft robotic fish for 3D swimming*," *14th International Symposium on Experimental Robotics*, Marrakech and Essaouira, Morocco (Springer, 2016).
37. N. Kamamichi, M. Yamakita, K. Asaka and Z.-W. Luo, "A snake-like swimming robot using IPMC actuator/sensor," *Proceedings of 2006 IEEE International Conference on Robotics and Automation, ICRA,* Orlando, FL, USA (IEEE, 2006).
38. J. Zhao, X. Zhang and Q. Pan. "A water walking robot inspired by water strider," *IEEE International Conference on Mechatronics and Automation*, Chengdu, China (2012).
39. S. Seok, A. Wang, M. Y. Chuah, D. Otten, J. Lang and S. Kim, "Design principles for highly efficient quadrupeds and implementation on the MIT cheetah robot," *2013 IEEE International Conference on Robotics and Automation (ICRA)*, Karlsruhe, Germany (IEEE, 2013).
40. K. A. Daltorio, A. D. Horchler, S. Gorb, R. E. Ritzmann and R. D. Quinn, "A small wall-walking robot with compliant, adhesive feet," *2005 IEEE/RSJ International Conference on Intelligent Robots and Systems, (IROS 2005)*, Alberta, Canada (IEEE, 2005).
41. B. C. Mac Murray, C. C. Futran, J. Lee, K. W. O'Brien, A. A. Amiri Moghadam, B. Mosadegh, M. N. Silberstein, J. K. Min and R. F. Shepherd, "Compliant buckled foam actuators and application in patient-specific direct cardiac compression," *Soft Robot*. **5**(1), 99–108 (2018).
42. F. Esser, T. Steger, D. Bach, T. Masselter and T. Speck, "Development of novel foam-based soft robotic ring actuators for a biomimetic peristaltic pumping system," *Conference on Biomimetic and Biohybrid Systems,* Stanford, CA, USA (Springer, 2017).
43. C. Tang, B. Li, C. Bian, Z. Li, L. Liu and H. Chen, "A locomotion robot driven by soft dielectric elastomer resonator," *10th International Conference on Robotics and Automation (ICIRA)*, Wuhan, China (Springer, 2017).
44. Y. Maeda, N. Kodera and T. Egawa. "Caging-based grasping by a robot hand with rigid and soft parts," *2012 IEEE International Conference on Robotics and Automation (ICRA)*, St. Paul, Minnesota, USA (IEEE, 2012).

45. J. D. Tedford, "Developments in robot grippers for soft fruit packing in New Zealand," *Robotica* **8**(4), 279–283 (1990).
46. K. C. Galloway, K. P. Becker, B. Phillips, J. Kirby, S. Licht, D. Tchernov, R. J. Wood and D. F. Gruber, "Soft robotic grippers for biological sampling on deep reefs," *Soft Robot*. **3**(1), 23–33 (2016).
47. T. Buschmann, S. Lohmeier, H. Ulbrich and F. Pfeiffer, "Dynamics simulation for a biped robot: Modeling and experimental verification," *2006 IEEE International Conference on Robotics and Automation (ICRA)*, Orlando, Florida, USA (IEEE, 2006).
48. O. Unver and M. Sitti. "A miniature ceiling walking robot with flat tacky elastomeric footpads," *IEEE International Conference on Robotics and Automation (ICRA)*, Kobe, Japan (IEEE, 2009).
49. J. Xiao, B. Li, K. Ushiroda and Q. Song, "Rise-rover: A wall-climbing robot with high reliability and load-carrying capacity," *2015 IEEE International Conference on Robotics and Biomimetics (ROBIO),* Zhuhai, China (IEEE, 2015).
50. R. M. Voyles, "TerminatorBot: A robot with dual-use arms for manipulation and locomotion," *IEEE International Conference on Robotics and Automation (ICRA),* San Francisco, CA, USA (IEEE, 2000).
51. B. Li, K. Ushiroda, L. Yang, Q. Song and J. Xiao, "Wall-climbing robot for non-destructive evaluation using impact-echo and metric learning SVM," *Int. J. Intel. Robot. Appl*. **1**(3), 255–270 (2017).
52. I. M. Van Meerbeek, B. C. Mac Murray, J. W. Kim, S. S. Robinson, P. X. Zou, M. N. Silberstein and R. F. Shepherd, "Morphing metal and elastomer bicontinuous foams for reversible stiffness, shape memory, and self-healing soft machines," *Adv. Mater*. **28**(14), 2801–2806 (2016).
53. N. G. Cheng, A. Gopinath, L. Wang, K. Iagnemma and A. E. Hosoi, "Thermally tunable, self-healing composites for soft robotic applications," *Macromol. Mater. Eng.* **299**(11), 1279–1284 (2014).
54. A. Argiolas, B. C. Mac Murray, I. Van Meerbeek, J. Whitehead, E. Sinibaldi, B. Mazzolai and R. F. Shepherd, "Sculpting soft machines," *Soft Robot*. **3**(3), 101–108 (2016).
55. M. P. Michalowski, S. Sabanovic and P. Michel, "Roillo: Creating a social robot for playrooms," *15th IEEE International Symposium on Robot and Human Interactive Communication (ROMAN),* Hatfield, United Kingdom (IEEE, 2006).
56. C. M. Donatelli, Z. T. Serlin, P. Echols-Jones, A. E. Scibelli, A. Cohen, J.-M. Musca, S. Rozen-Levy, D. Buckingham, R. White and B. A. Trimmer, "Soft foam robot with caterpillar-inspired gait regimes for terrestrial locomotion," *2017 IEEE/RSJ International Conference on Intelligent Robots and Systems (IROS),* Vancouver, Canada (IEEE, 2017).
57. J. Bruce, K. Caluwaerts, A. Iscen, A. P. Sabelhaus and V. SunSpiral, "Design and evolution of a modular tensegrity robot platform," *2014 IEEE International Conference on Robotics and Automation (ICRA),* Hong Kong, China (IEEE, 2014).
58. J. Bruce, A. P. Sabelhaus, Y. Chen, D. Lu, K. J. Morse, S. Milam, K. Caluwaerts, A. M. Agogino and V. SunSpiral, "SUPERball: Exploring tensegrities for planetary probes," *12th International Symposium on Artificial Intelligence, Robotics and Automation in Space (i-SAIRAS)*, Montreal, Canada (2014).
59. L.-H. Chen, M. C. Daly, A. P. Sabelhaus, L. A. J. van Vuuren, H. J. Garnier, M. I. Verdugo, E. Tang, C. U. Spangenberg, F. Ghahani, A. M. Agogino and A. K. Agogino, "Modular elastic lattice platform for rapid prototyping of tensegrity robots," *2017 International Design Engineering Technical Conferences and Computers and Information in Engineering Conference,* Cleveland, Ohio (ASME, 2017).
60. S. H. Juan and J. M. M. Tur, "Tensegrity frameworks: Static analysis review," *Mech. Mach. Theory* **43**(7), 859–881 (2008).
61. R. T. Skelton and C. Sultan, "Controllable tensegrity: A new class of smart structures," **In**: *Smart Structures and Materials 1997: Mathematics and Control in Smart Structures*. (International Society for Optics and Photonics, San Diego, CA, USA, 1997).
62. J. M. M. Tur and S. H. Juan, "Tensegrity frameworks: Dynamic analysis review and open problems," *Mech. Mach. Theory*. **44**(1), 1–18 (2009).
63. D. Zappetti, S. Mintchev, J. Shintake and D. Floreano, "Bio-inspired tensegrity soft modular robots," *Conference on Biomimetic and Biohybrid Systems,* Stanford, CA, USA (Springer, 2017).
64. M. Johnson, Y. Chen, S. Hovet, S. Xu, B. J. Wood, H. Ren, J. Tokuda, Z. T. H. Tse, "Fabricating biomedical origami: A state-of-the-art review," *Int. J. Comput. Assist. Radiol. Surg*. **12**(11), 2023–2032 (2017).
65. A. Lebée, "From folds to structures, a review," *Int. J. Space Struct*. **30**(2), 55–74 (2015).
66. E. Morris, D. A. McAdams and R. Malak, "The state of the art of origami-inspired products: A review," *2016 International Design Engineering Technical Conferences and Computers and Information in Engineering Conference*, Charlotte, NC, USA (ASME, 2016).
67. E. A. Peraza-Hernandez, D. J. Hartl, R. J. Malak Jr and D. C. Lagoudas, "Origami-inspired active structures: A synthesis and review," *Smart Mater. Struct*. **23**(9), 094001 (2014).
68. A. Rafsanjani and K. Bertoldi, "Buckling-induced kirigami," *Phys. Rev. Lett*. **118**(8), 084301 (2017).
69. A. Rafsanjani, Y. Zhang, B. Liu, S. M. Rubinstein and K. Bertoldi, "Kirigami skins make a simple soft actuator crawl," *Sci. Robot*. **3**(15), eaar7555 (2018).
70. M. Cianchetti, T. Ranzani, G. Gerboni, T. Nanayakkara, K. Althoefer and P. Dasgupta, "Soft robotics technologies to address shortcomings in today's minimally invasive surgery: The STIFF-FLOP approach," *Soft Robot*. **1**(2), 122–131 (2014).
71. W. Wang, N.-G. Kim, H. Rodrigue and S.-H. Ahn, "Modular assembly of soft deployable structures and robots," *Mater. Horiz.* **4**(3), 367–376 (2017).
72. M. Yim, W.-M. Shen, B. Salemi, D. Rus, M. Moll, H. Lipson, E. Klavins and G. S. Chirikjian, "Modular self-reconfigurable robot systems [grand challenges of robotics]," *IEEE Robot Autom. Mag*. **14**(1), 43–52 (2007).

73. L. J. Gibson and M. F. Ashby, *Cellular Solids: Structure and Properties* (Cambridge University Press, Cambridge, UK, 1999).
74. S. Ouellet, D. Cronin and M. Worswick, "Compressive response of polymeric foams under quasi-static, medium and high strain rate conditions," *Polym. Test*. **25**(6), 731–743 (2006).
75. J. Zhang, Z. Lin, A. Wong, N. Kikuchi, V. C. Li, A. F. Yee and G. S. Nusholtz, "Constitutive modeling and material characterization of polymeric foams," *J. Eng. Mater. Tech.* **119**(3), 284–291 (1997).
76. M. F. Ashby and R. M. Medalist, "The mechanical properties of cellular solids," *Metall. Trans. A* **14**(9), 1755–1769 (1983).
77. D. G. Piero and G. Pampolini, "On the rate-dependent properties of open-cell polyurethane foams," *1st International Conference on Material Modelling (ICMM)*, Westfalenhallen Dortmund, Germany (2009).
78. O. Faruque, N. N. Liu and C. C. Chou, "Strain rate dependent foam-constituitive modeling and applications," SAE Technical Paper (1997).
79. K. Suzumori, S. Iikura and H. Tanaka, "Development of flexible microactuator and its applications to robotic mechanisms," *1991 IEEE International Conference on Robotics and Automation (ICRA)*, Sacramento, CA, USA (IEEE, 1991).
80. B. Mosadegh, P. Polygerinos, C. Keplinger, S. Wennstedt, R. F. Shepherd, U. Gupta, J. Shim, K. Bertoldi, C. J. Walsh and G. M. Whitesides, "Pneumatic networks for soft robotics that actuate rapidly," *Adv. Funct. Mater*. **24**(15), 2163–2170 (2014).
81. R. F. Shepherd, A. A. Stokes, J. Freake, J. Barber, P. W. Snyder, A. D. Mazzeo, L. Cademartiri, S. A. Morin and G. M. Whitesides, "Using explosions to power a soft robot," *Angew. Chem*. **125**(10), 2964–2968 (2013).
82. S. Seok, C. D. Onal, K.-J. Cho, R. J. Wood, D. Rus and S. Kim, "Meshworm: A peristaltic soft robot with antagonistic nickel titanium coil actuators," *IEEE/ASME Trans. Mech.* **18**(5), 1485–1497 (2013).
83. H.-T. Lin, G. Leisk and B. A. Trimmer, "GoQBot: A caterpillar-inspired soft-bodied rolling robot," *Bioinspir. Biomim*. **6**(2), 026007–21 (2011).
84. Y. Bahramzadeh and M. Shahinpoor, "A review of ionic polymeric soft actuators and sensors," *Soft Robot*. **1**(1), 38–52 (2014).
85. F. Carpi, R. Kornbluh, P. Sommer-Larsen and G. Alici, "Electroactive polymer actuators as artificial muscles: Are they ready for bioinspired applications?" *Bioinspir. Biomim*. **6**(4), 045006 (2011).
86. F. Renda, M. Cianchetti, M. Giorelli, A. Arienti and C. Laschi, "A 3D steady-state model of a tendon-driven continuum soft manipulator inspired by the octopus arm," *Bioinspir Biomim*. **7**(2), 025006 (2012).
87. M. W. Hannan and I. D. Walker, "Kinematics and the implementation of an elephant's trunk manipulator and other continuum style robots," *J. Robot. Syst*. **20**(2), 45–63 (2003).
88. H. T. Lin and B. A. Trimmer, "The substrate as a skeleton: Ground reaction forces from a soft-bodied legged animal," *J. Exp. Biol*. **213**(7), 1133–1142 (2010).
89. Y.-L. Park, B.-R. Chen, N. O. Pérez-Arancibia, D. Young, L. Stirling, R. J. Wood, E. C. Goldfield and R. Nagpal, "Design and control of a bio-inspired soft wearable robotic device for ankle? Foot rehabilitation," *Bioinspir. Biomim*. **9**(1), 016007 (2014).
90. V. Vikas, E. Cohen, R. Grassi, C. Sozer and B. Trimmer, "Design and locomotion control of soft robot using friction manipulation and motor-tendon actuation," *IEEE Transactions on Robotics* **32** (4), 949–959 (2016).
91. C. Laschi, B. Mazzolai, V. Mattoli, M. Cianchetti and P. Dario, "Design of a biomimetic robotic octopus arm," *Bioinspir. Biomim*. **4**(1), 015006 (2009).
92. V. Vikas, P. Grover and B. Trimmer, "Model-free control framework for multi-limb soft robots," *2015 IEEE/RSJ International Conference on Intelligent Robots and Systems (IROS),* Hamburg, Germany (IEEE, 2015).
93. T. Umedachi, V. Vikas and B. A. Trimmer, "Highly deformable 3-d printed soft robot generating inching and crawling locomotions with variable friction legs," *2013 IEEE/RSJ International Conference on Intelligent Robots and Systems (IROS)*, Tokyo, Japan (IEEE, 2013).